Materials Advances

ROYAL SOCIETY OF CHEMISTRY

COMMUNICATION

View Article Online
View Journal | View Issue

Cite this: *Mater. Adv.*, 2025, 6, 552

Received 19th September 2024,
Accepted 3rd December 2024

DOI: 10.1039/d4ma00947a

rsc.li/materials-advances

Stabilization of nesquehonite for application in carbon capture utilization and storage†

Nirrupama Kamala Ilango, [a] Hoang Nguyen, [a] Mohammad Alzeer, [a]‡ Frank Winnefeld [b] and Paivo Kinnunen [a]*

Nesquehonite ($MgCO_3·3H_2O$) is of interest as a carbon sink for mineral carbonation as its formation is kinetically favored at ambient temperatures and pressures and offers the highest CO_2 : MgO ratio compared to most other hydrated magnesium carbonates (HMCs). However, the phase tends to convert to more stable HMCs depending on the environment and time leading to long-term instability. Here, we report a successful attempt to stabilize nesquehonite using a phosphate-based pH 7 buffer, while controlling the equilibrium of aqueous carbonate species did not stabilize the phase. Phosphate interacts with nesquehonite to form a Mg-phosphate phase on nesquehonite's surface. We suggest that a protective layer is formed, which prevents further transformation of nesquehonite.

Introduction

Mineral carbonation of Ca/Mg-rich rocks has been considered a safe and promising method to capture CO_2 in solid form.[1,2] The estimated availability of ultramafic magnesium silicates including serpentine ($(Mg,Fe)_3Si_2O_5(OH)_4$) and olivine ($(Mg,Fe)_2SiO_4$) accounts for over 10 000 billion tons worldwide[3] offering great potential for a permanent carbon sink as magnesium carbonates. To sequestrate all of the anthropogenic CO_2 emissions for the next 1000 years, considering an emission of about 50 billion tons per year, a fraction of these deposits would be sufficient.[4] As the economic viability of such processes for large-scale carbon capture utilization and storage (CCUS) is dependent on waste-free processes and extra revenue from selling their output, viable utilization of these carbonated phases is essential to enable the scalability of CCUS.

Magnesite ($MgCO_3$) is the most stable magnesium carbonate in the $MgO–CO_2–H_2O$ system and is an ideal carbon sink; however, it requires elevated temperatures and pressures to precipitate. However, a range of metastable hydrated magnesium carbonates (HMCs) are formed depending on the reaction conditions.[5] For instance, nesquehonite ($MgCO_3·3H_2O$) readily forms by the addition of $MgCl_2$ solution to an aqueous solution of Na_2CO_3 at ambient conditions of 25 °C and 1 bar P_{CO_2}, while it takes about 5–15 hours at 120 °C and 3 bar P_{CO_2} for magnesite precipitation with hydromagnesite ($Mg_5(CO_3)_4(OH)_2·4H_2O$) as an intermediate.[6] This makes nesquehonite an attractive product of several CCUS processes.[7,8] Furthermore, it finds application in the production of low-CO_2 construction materials such as gypsum-like products[9] and thermal energy storage.[10] Hydrated magnesium carbonates also have great potential as an alternative to conventional cement.[11]

The bottleneck in using nesquehonite in such applications is the stability of the phase as it transforms to thermodynamically more stable HMCs with a change in temperature, pH, CO_2 concentration, water saturation, and/or aging.[7,12,13] This phase transformation is accompanied by a large decrease in volume[14] leading to structural instability and some loss of CO_2. The transformation pathways of nesquehonite with temperature have been studied extensively. At 0 K, the free energy of formation of nesquehonite (−245.46 kJ mol^{-1} from oxides) is much lower than for hydromagnesite (−139.33 kJ mol^{-1}) and magnesite (−114.14 kJ mol^{-1}) indicating high stability; however, the phase becomes less stable with increase in temperature.[15] Early studies have shown that in an aqueous medium, the phase starts decomposing at around 50 °C to hydromagnesite through various intermediates, such as amorphous magnesium carbonates and dypingite ($Mg_5(CO_3)_4(OH)_2·5–8H_2O$).[5,12,16] However, recent calculations from thermodynamic data show that the transition occurs at much lower temperatures (see Fig. S1 in the ESI†).[17] To date, there are not many attempts to stabilize nesquehonite reported in the

[a] *Fibre and Particle Engineering Research Unit, University of Oulu, Pentti Kaiteran katu 1, 90014 Oulu, Finland. E-mail: paivo.kinnunen@oulu.fi*
[b] *Swiss Federal Laboratories for Material Science and Technology (Empa), Laboratory for Concrete & Asphalt, Überlandstrasse 129, 8600 Dübendorf, Switzerland*

† Electronic supplementary information (ESI) available. See DOI: https://doi.org/10.1039/d4ma00947a

‡ Current address: Department of Chemistry, University of Helsinki A.I. Virtasenaukio 1, Helsinki 00014, Finland.

literature, and the mechanism and pathway to stabilize the phase remain unclear.[18]

The chemical formula of nesquehonite has been a subject of open debate in the literature, some favoring the presence of bicarbonate $Mg(HCO_3)(OH)\cdot 2H_2O$[19] in contrast to carbonate $MgCO_3\cdot 3H_2O$[20,21] in the structure. Here, we do not intend to contribute to this debate, but consider the possibility of the existence of either bicarbonate (HCO_3^-) or carbonate (CO_3^{2-}) ions in the crystal. Therefore, the equation, $HCO_3^- \leftrightarrow CO_3^- + H^+$ may play a vital role in regulating the stability of nesquehonite. The equilibrium of the solution shifts towards carbonate with the increase in temperature and pH (Fig. S2 in ESI†). Furthermore, the transformation of nesquehonite to dypingite and/or hydromagnesite, both these minerals host carbon in the form of carbonates in the structure, is accelerated with increase in temperature and is accompanied by a shift in the solution equilibrium from bicarbonate to carbonate, which is known to be a temperature-dependent relation.[22] Here, we hypothesize that the stability of nesquehonite is connected to the solution equilibrium between bicarbonate and carbonate ions, which drives the conversion of nesquehonite to other HMCs *via e.g.*, temperature increase. In that case, nesquehonite could be stabilized by regulating the equilibrium between bicarbonates and carbonates. Thus, to test this hypothesis, we experimentally validate whether nesquehonite is stabilized at elevated temperatures by shifting the solution equilibrium towards bicarbonate through three approaches:

1. By increasing the carbonate ion concentration with the addition of sodium carbonate solutions of different molar concentrations.

2. By protonation; adding hydrochloric acid as the source of H^+.

3. Using a pH 7 buffer solution to maintain the pH of the solution at 7 to have mainly bicarbonate speciation.

The precipitates were collected after several days and were analyzed for phase composition using various analytical techniques (see Methods in the ESI†). In further experiments, we investigated the effect of several pH buffers with different compositions on the stability of nesquehonite to further investigate the mechanisms of nesquehonite stabilization.

Methodology

Na_2CO_3 solutions of three different concentrations (0.01 M, 0.05 M, and 0.1 M), and 0.1 M HCl solution were prepared using Milli-Q water and were left to equilibrate for 24 hours. A commercially available phosphate-based buffer of pH 7.00 ± 0.02 (20 °C) was used for the study (referred to as pH 7 (CB)). Two different pH 7 buffers, one based on potassium dihydrogen phosphate (KH_2PO_4) and sodium hydroxide (NaOH) referred to as pH 7-phosphate and the other based on tris(hydroxymethyl)aminomethane ($(HOCH_2)_3CNH_2$) and hydrochloric acid (HCl) referred to as pH 7-amine, were prepared in the laboratory (for more details see Methods in the ESI†). The buffer solutions were left to equilibrate for 24 hours before the experiments. The pH values, as measured using a Hach pH electrode, of the phosphate-based and amine-based buffers were 7.10 and 7.11, respectively. The accuracy in the pH measurement was <0.1 pH units. Nesquehonite was synthesized in the laboratory by bubbling CO_2 into an aqueous $Mg(OH)_2$ solution (see Fig. S3, Methods in ESI†). For the first test series, 1 g of the synthesized nesquehonite was added to 10 ml of the prepared solutions of Na_2CO_3, HCl and pH 7 (CB). The mix was left to equilibrate at 50 °C for 10 days. The temperature was chosen to accelerate the phase transformation of nesquehonite. Afterwards, the solids were gained by vacuum filtration, washed with isopropanol followed by diethyl ether, and dried at 40 °C for 30 min. Before further analysis, the precipitates were ground gently with a mortar and pestle and passed through a 63 μm sieve. For the second test series, nesquehonite (1 g) was added to 10 ml of the lab-made and commercial pH 7 buffers. A reference of nesquehonite mixed in Milli-Q water was also prepared for comparison. All suspensions were kept at 50 °C for 7 and 28 days, after which the filtration was done as previously described.

The role of solution equilibrium between the carbonate species

The synthesized nesquehonite exhibits the typical prismatic needle-like shape (Fig. 1a). The morphologies of the precipitates aged in pH 7 buffer (CB), 0.1 M hydrochloric acid, and 0.1 M sodium carbonate are shown in Fig. 1b–d, respectively. In the pH 7 buffer (CB), precipitation of a phase on the nesquehonite surface can be observed. However, in the hydrochloric acid and sodium carbonate solutions, a house of card texture forming at the expense of nesquehonite indicates the presence of a dypingite-like phase.[13] In these two samples, the conversion of nesquehonite to dypingite is confirmed by the X-ray diffraction patterns of the precipitates (Fig. 2). Reflections at 6.60° (15.53 Å), 10.04° (10.22 Å), 16.03° (6.41 Å) and 17.63° (5.83 Å) 2θ CoKα are observed indicating the presence of dypingite in 0.1 M HCl and Na_2CO_3 solutions. Similar results

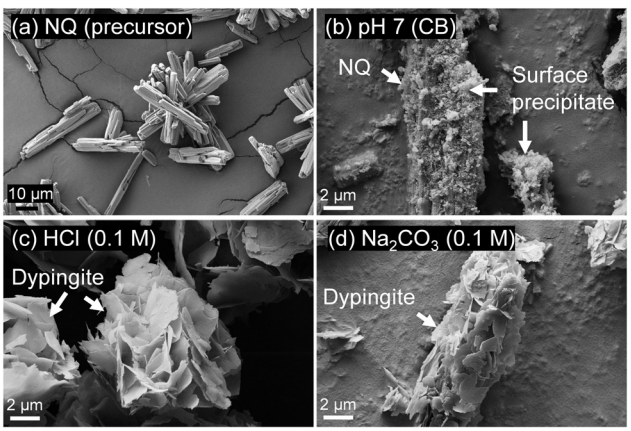

Fig. 1 (a) Needle-like morphology of nesquehonite, (b)–(d) morphology of the precipitates after 10 days at 50 °C: (b) in pH 7 buffer solution CB, (c) in 0.1 M HCl and (d) in 0.1 M sodium carbonate. NQ = nesquehonite.

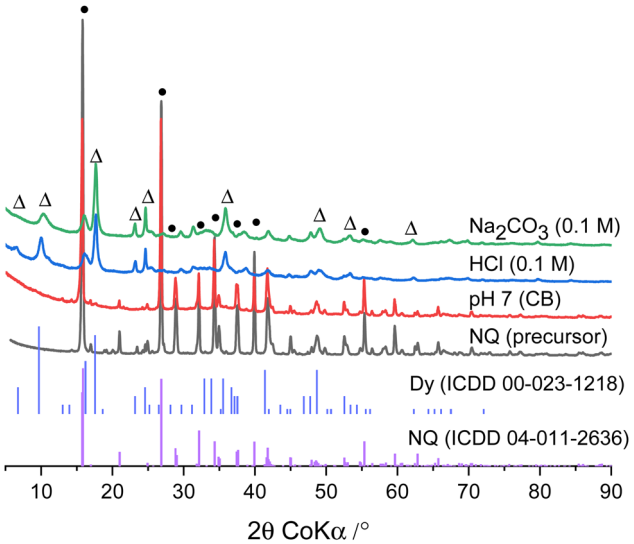

Fig. 2 X-ray diffraction pattern of the nesquehonite (NQ) precursor and the precipitates formed after 10 days at 50 °C. The diffraction patterns of nesquehonite and dypingite (D_y) from the ICDD database are plotted for reference. Nesquehonite is indicated as • and dypingite as Δ.

are observed for lower concentrations of sodium carbonate (Fig. S4 in ESI†).

The characteristic reflections of nesquehonite at 15.80° (6.50 Å), 21.01° (4.90 Å), 26.86° (3.85 Å), 32.16° (3.22 Å) 2θ CoKα are present in the sample stored in the pH 7 buffer solution (CB). A broad hump between 25–42° 2θ CoKα is also observed and could indicate the presence of amorphous phases. From the results, it is evident that in the pH 7 buffer solution (CB), nesquehonite remains stable even after 10 days at 50 °C, while it transforms to dypingite in the case of sodium carbonate or hydrochloric acid. The pH of the solutions after 10 days is measured to be 9.21, 8.30 and 9.52 in pH 7 (CB), 0.1 M HCl and 0.1 M Na_2CO_3, respectively. It can be observed that the phase transformation occurs at a pH of 8.30 and 9.52, but not at the intermediate pH of 9.21, suggesting that there should be other potential reason for the observed phenomenon. Thus, we postulate that the phosphate in the commercial buffer could be the reason and not the pH of the solution. To confirm the effect of the anion in stabilizing nesquehonite, further experiments were conducted with pH 7 buffers prepared with (pH-7 (CB) and phosphate) and without phosphate (pH 7-amine).

The interaction of phosphate with nesquehonite

Fig. 3a shows the diffraction patterns of nesquehonite in Milli-Q water and in the buffer solutions with and without phosphate after 28 days at 50 °C. Similar results are observed after 7 days and are shown in Fig. S5 in the ESI.† The transformation of nesquehonite to dypingite is observed in the reference system (Milli-Q water) as expected. In the case of phosphate-based pH 7 buffers, both commercial and lab-made, nesquehonite is still present after 28 days of reaction. The hump between 25–42° 2θ CoKα as observed previously after 10 days is also present. However, this is not the case for the pH 7 buffer prepared with tris(hydroxymethyl)aminomethane and hydrochloric acid. No reflections of nesquehonite are observed due to the transformation to dypingite.

The thermal decomposition of the precipitates (Fig. 3b) as measured by thermogravimetry also confirms these findings. The mass losses at 110, 160 and 220 °C of the solids stored in pH 7 (CB) and pH 7-phosphate samples indicate the dehydration of nesquehonite. The decarbonation occurs at 440 and 485 °C, similar to results reported elsewhere.[23] For the

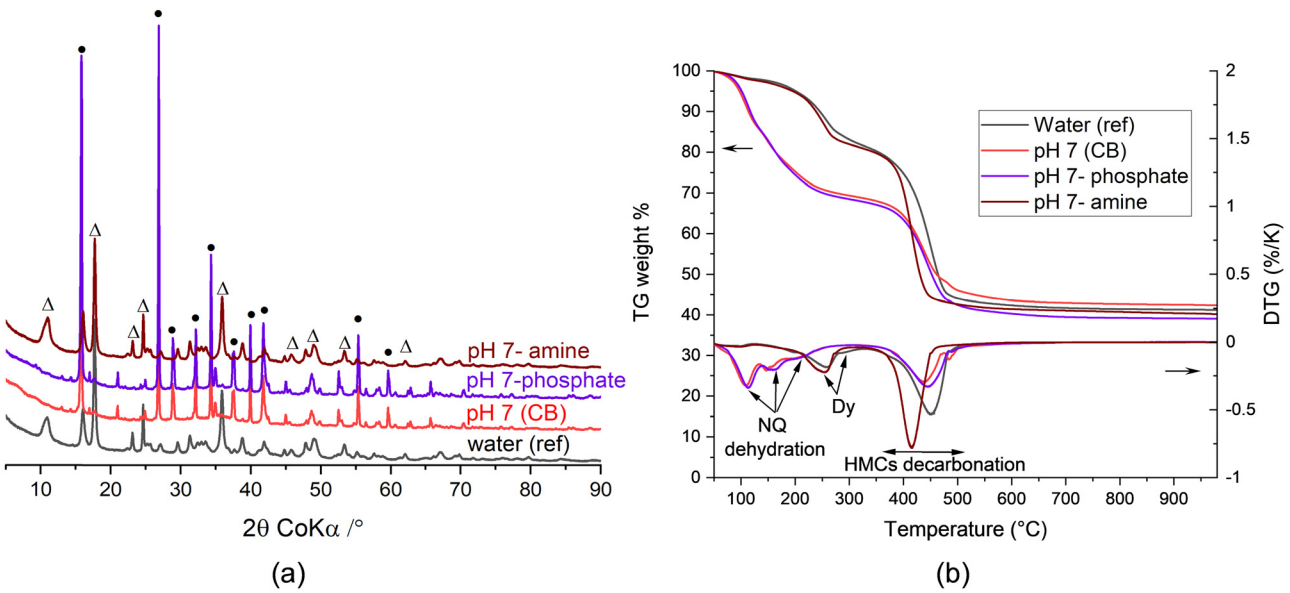

Fig. 3 (a) X-ray diffraction pattern and (b) thermogravimetry of nesquehonite stored in water and pH buffer solutions at 50 °C for 28 days. Nesquehonite is indicated as • or NQ and dypingite as Δ or Dy.

reference and pH 7-amine samples dehydration occurs around 250 °C, dehydroxylation at about 300 °C and decarbonation at 450 °C and 415 °C, respectively. The total mass losses of 58.7% and 59.7% for the reference and pH 7-amine, respectively, are close to the theoretical mass loss of dypingite (58.5%).[24] The amount of nesquehonite after 28 days is quantified considering the mass loss around 350–600 °C due to the decarbonation of nesquehonite (see Methods in ESI†). About 80% and 86% of nesquehonite remained after 28 days in pH 7(CB) and pH 7-phosphate, respectively, which is similar to the values after 7 days. This indicates that the phase is stable at 50 °C up to 28 days. In conclusion, the effect of pH is not the primary factor that prevents the phase transformation, but the interaction between the phosphate-based buffer and nesquehonite resulting in the formation of a precipitate on the surface of nesquehonite (see Fig. S6 in the ESI†), potentially inhibiting further reaction.

Fig. 4a shows the EDS mapping done on precipitates after 28 days in pH 7-phosphate. The nesquehonite mineral is surrounded by phosphate and potassium rich phases. From thermodynamic calculations using GEMS, bobierrite ($Mg_3(PO_4)_2{\cdot}8H_2O$) is predicted to be the stable magnesium phosphate that formed in this system (Fig. S7 in ESI†); this phase might be similar in bulk composition to the phase observed experimentally *via* SEM on the surface of nesquehonite. The broad hump in XRD between 25–42° 2θ CoKα (Fig. 3a) may indicate the presence of an amorphous magnesium potassium phosphate (MKP) phase. Experimental evidence has shown that the crystallization of MKP phases from MgO occurs from the formation of intermediate amorphous phases.[25] Furthermore, the dehydration of MKP phases occurs around 70–250 °C and strongly overlaps with that of nesquehonite. However, the mass losses around 65, 110 and 150 °C, see Fig. 3b, possibly corresponding to the dehydration of $Mg_2KH(PO_4)_2{\cdot}15H_2O$, K-struvite and bobierrite, respectively,[26] tentatively indicate the presence of more than one MKP phase. Also, from the ternary diagram obtained from the EDS map (Fig. 4b), a strong intermixing between nesquehonite and the MKP phases close to the compositions of $Mg_2KH(PO_4)_2{\cdot}15H_2O$ and $MgKPO_4{\cdot}6H_2O$ (K-struvite) can be seen. This is a further indication that they form on the nesquehonite surface. Therefore, the results suggest that the tendency of the magnesium ions to complex with both phosphate and carbonate ions at the relevant pH of about 9.2 (as calculated by GEMS, see Fig. S8 in the ESI†) results in the formation of magnesium phosphate phases on the surface.

Conclusions

In an attempt to stabilize nesquehonite and prevent its conversion to other HMCs such as dypingite or hydromagnesite, the solution equilibrium was tuned to favor the formation of bicarbonate ions. It was observed that a phosphate-based pH 7 buffer was successful in preventing the phase transformation, but other ways to increase bicarbonate concentration with the addition of Na_2CO_3 and HCl failed. Moreover, we hypothesize that the pH might not be the reason for the stability of the phase; instead, the type of ligand matters. To confirm this, the experiments were repeated using two custom-made pH 7 buffers, one containing phosphate, and one without phosphate. The results indicated that the interaction between the phosphate and magnesium forms a magnesium potassium phosphate (MKP) phase on the surface of the nesquehonite crystals, which may act as a protective layer hindering further reaction. This MKP phase is X-ray amorphous with a bulk chemical composition in between various MKP phases such as bobierrite, K-struvite and $Mg_2KH(PO_4)_2{\cdot}15H_2O$.

The findings reported here show a possible way to stabilize nesquehonite for safe use in various CCUS processes where poor stability of the phase has been a major hurdle for its

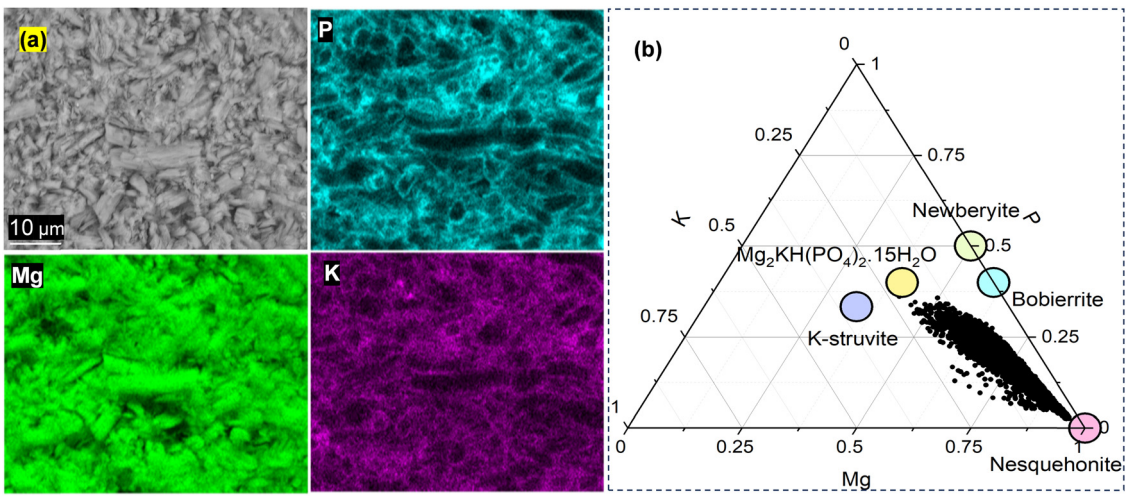

Fig. 4 (a) SEM-BSE image and EDS mapping of nesquehonite in lab-made phosphate buffer after 28 days. (b) Atomic ratio plots from EDS mapping for the ternary diagram Mg–K–P along with the theoretical atomic ratios of nesquehonite and various MKP phases.

utilization. For instance, considering its application as a construction material, the phase conversion from nesquehonite to dypingite would result in a 40% decrease in the solid volume as calculated from the molar volume of both phases[14] and some loss in CO_2. This could lead to cracks and destabilization in the long-term posing serious issues in structural applications. Here, we show that the use of phosphate effectively prevents nesquehonite conversion by about 80–85% under the investigated conditions. Further investigations are required to maximize the efficiency of the system by optimizing the Mg/P ratio, thereby preventing the loss of CO_2. The effect of higher temperatures and longer curing time needs to be looked at along with alternatives to phosphate, given its application as a fertilizer.

Author contributions

All: conceptualization, methodology, writing – review & editing, NI, HN, FW, PK: formal analysis, investigation, NI: writing – original draft, HN, FW, PK: supervision, PK: funding acquisition.

Data availability

Data for this article, including the raw files from XRD, TGA, EDS mapping and thermodynamic modelling are available at Zenodo at **https://doi.org/10.5281/zenodo.13709632**. Some of the data supporting this article have been included as part of the ESI.†

Conflicts of interest

There are no conflicts to declare.

Acknowledgements

The authors acknowledge the financial support from the University of Oulu & the Research Council of Finland (Profi5 326291, project 354767 and project 329477). The authors thank Durgaprasad Ramteke for TGA measurement and the Centre for Material Analysis, University of Oulu, Finland.

References

1 H. Haywood, J. Eyre and H. Scholes, *Environ. Geol.*, 2001, **41**, 11–16.
2 M. Mazzotti, J. C. Abanades, R. Allam, K. S. Lackner, F. Meunier, E. Rubin, J. C. Sanchez, K. Yogo and R. Zevenhoven, *IPCC Special report on carbon dioxide capture and storage*, Cambridge University Press, 2005.
3 C. Unluer, in *Carbon Dioxide Sequestration in Cementitious Construction Materials*, eds. F. Pacheco-Torgal, C. Shi and A. P. Sanchez, Woodhead Publishing, 2018, pp. 129–173.
4 A. Scott, C. Oze, V. Shah, N. Yang, B. Shanks, C. Cheeseman, A. Marshall and M. Watson, *Commun. Earth Environ.*, 2021, **2**, 1–6.
5 M. Liska, A. Wilson and J. Bensted, in *Lea's Chemistry of Cement and Concrete*, eds. P. C. Hewlett and M. Liska, Butterworth-Heinemann, 2019, pp. 585–640.
6 M. Hänchen, V. Prigiobbe, R. Baciocchi and M. Mazzotti, *Chem. Eng. Sci.*, 2008, **63**, 1012–1028.
7 A. Entezari Zarandi, F. Larachi, G. Beaudoin, B. Plante and M. Sciortino, *Chem. Eng. J.*, 2017, **314**, 160–168.
8 G. Gadikota, *Commun. Chem.*, 2021, **4**, 23.
9 F. P. Glasser, G. Jauffret, J. Morrison, J.-L. Galvez-Martos, N. Patterson and M. S.-E. Imbabi, *Front. Energy Res.*, 2016, **4**, 3.
10 R. Erlund and R. Zevenhoven, *J. Energy Storage*, 2019, **25**, 100907.
11 E. Bernard, H. Nguyen, S. Kawashima, B. Lothenbach, H. Manzano, J. Provis, A. Scott, C. Unluer, F. Winnefeld and P. Kinnunen, *RILEM Tech. Lett.*, 2023, **8**, 65–78.
12 P. J. Davies and B. Bubela, *Chem. Geol.*, 1973, **12**, 289–300.
13 L. Hopkinson, P. Kristova, K. Rutt and G. Cressey, *Geochim. Cosmochim. Acta*, 2012, **76**, 1–13.
14 E. Bernard, B. Lothenbach, D. Rentsch, A. German and F. Winnefeld, *Mater. Struct.*, 2022, **55**, 183.
15 A. M. Chaka and A. R. Felmy, *J. Phys. Chem. A*, 2014, **118**, 7469–7488.
16 D. Langmuir, *J. Geol.*, 1965, **73**, 730–754.
17 B. Lothenbach, E. Bernard, A. German and F. Winnefeld, *Papers*, 2023, **6**, 342–356.
18 R. Pokharel, I. C. Popa, Y. de Kok and H. E. King, *Environ. Sci. Technol.*, 2024, **58**, 362–370.
19 R. L. Frost and S. J. Palmer, *Spectrochim. Acta, Part A*, 2011, **78**, 1255–1260.
20 F. A. Genth and S. L. Penfield, *Am. J. Sci.*, 1890, **3–39**, 121–137.
21 J. Cui, T. R. Prisk, D. L. Olmsted, V. Su, M. Asta and S. E. Hayes, *Chem. – Eur. J.*, 2023, **29**, e202203052.
22 R. S. Gärtner and G.-J. Witkamp, *Hydrometallurgy*, 2007, **88**, 75–91.
23 G. Jauffret, J. Morrison and F. P. Glasser, *J. Therm. Anal. Calorim.*, 2015, **122**, 601–609.
24 G. Yamamoto, A. Kyono and S. Okada, *Mater. Lett.*, 2022, **308**, 131125.
25 A. Viani and P. Mácová, *CrystEngComm*, 2018, **20**, 4600–4613.
26 B. Xu, B. Lothenbach and Z. Li, *Cem. Concr. Compos.*, 2022, **134**, 104807.